EFFICIENT PARAMETERIZATION OF THERMO-ELASTIC CORRECTION MODELS FOR EXTERNALLY DRIVEN SPINDLES

CHRISTIAN BRECHER, ALEXANDER STEINERT, ROBERT SPIERLING, STEPHAN NEUS

Laboratory for Machine Tools and Production Engineering (WZL) of RWTH Aachen University, Germany

DOI : 10.17973/MMSJ.2021_03_2020076

A.Steinert@wzl.rwth-aachen.de

In modern machine tools, spindle units significantly contribute to thermo-elastic tool center point (TCP) errors. Correction models to compensate axial spindle expansion are currently based on linear temperature models. Despite existing expert knowledge of spindle manufacturers, considerable modelling effort and empirical studies are required to parametrize appropriate models. As a result, the experimental effort is often reduced to a small number of load cases leading to limited accuracy over the entire range of applications.

The goal of this work is to reduce the current experimental effort for parameterization of thermo-elastic correction models to a minimum by parametrizing delay elements with a thermo-elastic spindle simulation. In consequence, the required experimental effort can be substituted by bearing friction tests.

KEYWORDS

thermal issues, thermal error compensation, spindle, thermo-elastic simulation

1 INTRODUCTION

Due to increasing power densities and energy consumptions, thermo-elastic effects increasingly affect the operating conditions of modern machine tools. In order to reduce the impact of thermo-elastic deformations on the achievable accuracy, correction models are used to compensate respective deformations by adjusting axis positions. Thermo-elastic correction models for machine tool spindle units are often designed based on expert knowledge and empirical tests. Therefore, correlations of discrete structural temperature information and the desired axial shaft displacement are assumed.

In the past decades, extensive research work was conducted to model thermo-elastic behavior of machine tools and their components. Yet, only a few approaches were successfully applied in industry, since most models require a large parametrization effort on a machine tool.

2 STATE OF THE ART AND APPROACH

While the first paragraph of this chapter refers to the state of the art for spindle modelling, the second paragraph focusses on the correction of thermo-elastic spindle errors. The third paragraph deals with the research approach.

2.1 State of the art of thermo-elastic spindle modelling

Spindle systems of machine tools for metal cutting have already been examined in various studies. While Heisel [Heisel 2011] modelled the dynamic spindle behavior considering multi-dimensional bearing stiffness and damping characteristics, Gleich [Gleich 2008] and Hu [Hu 2013] developed promising approaches to illustrate the thermo-elastic behavior with reduced, fast-calculating models. Especially for high-speed applications, Kreis [Kreis 2008], Zahedi [Zahedi 2012] and Ma [Ma 2016] were able to identify and model mechanical and thermal interactions. In addition, Holkup presents an approach to simulate contact forces and spindle stiffness affected by transient thermal effects in [Holkup 2010]. Integrated thermo-mechanical spindle models considering nonlinear bearing preload were also developed in [Li 2004] and [Jedrzejewski 2008]. Furthermore, it was shown that detailed spindle models can provide a basis to increase the machining performance and accuracy [Kreis 2008, Gebert 1997].

In [Brecher 2020], a detailed FE-based white-box model is developed to predict thermo-mechanical interactions in externally driven spindles such as tool center point (TCP) deformations.

Heat generation in spindle bearings and the resulting temperatures of the bearing's outer and inner ring depend on spindle speed and load scenario. Therefore, spindle bearing characteristics are of central importance [Weck 2000].

Gebert [Gebert 1997] identified bearing friction and air friction between stationary and rotating spindle parts as the central heat sources in externally driven spindles. These effects can be investigated in experimental tests. Furthermore, friction models of Harris [Harris 1991], Steinert [Steinert 1995], Rossaint [Roissant 2013] or SKF [SKF 2013] allow calculating friction moments for different bearing geometries under external load.

2.2 State of the art correction of thermo-elastic errors

Thermo-elastic displacements can also be reduced by means of a correction procedure. There are different approaches to minimize spindle-induced misalignment based on internal control data. For respective correction models, spindle speed is mainly used as input variable. Linear [Heisel 1980], [Böttger 1994] and non-linear functions [Dehaes 1998], delay elements [Wuldsberg 1991], exponential functions [Spur 1986] and polynomial functions [Tönshoff 1990] serve to describe the thermo-elastic behavior of the spindle system. Tönshoff [Tönshoff 1990] and Wulfsberg [Wuldsberg 1991] also use the rotational speed as an input variable to calculate the displacement of the TCP and combine their approaches with a discontinuous direct displacement measurement. Heisel and Stehle [Heisel 1997] as well as Kim [Kim 2004] follow a similar approach and use both temperatures and rotational speed to approximate the thermo-elastic TCP behavior. Both approaches have in common that no external loads are considered.

In contrast to existing work, [Wissmann 2014] corrects the torque-related spindle load-dependent TCP displacement of a milling machine. Besides ambient temperature sensors, only control internal data are used for correction. Mares [Mares 2013] follows a similar modelling approach for the spindle-related components, but combines it with additional temperature information for the load-dependent components.

The mentioned correction methods are based on highly abstracted models and require complex experimental investigations to provide a profound database.

2.3 Research approach

The high parameterization effort due to complex thermo-elastic displacement tests on the machine tool is a major cost driver for an industrial implementation of these correction methods. The large number of influencing variables such as spindle speed, radial and axial load requires time-intensive test series for validation. Due to limited resources, a reduced test plan is often used which can only cover a small part of the relevant operating conditions. In consequence, the reduction of parametrization time results in a loss of correction quality. Furthermore, once parametrized correction models can not be applied to other machine-spindle combinations.

The goal of this research is to develop a methodology for the efficient parameterization of correction models by the example of an externally driven spindle. A virtual spindle prototype provides cost-effective thermo-elastic spindle deformations for a large spectrum of operating conditions. The virtual prototype in turn is based on a FE model that is connected to detailed part models describing thermal and mechanical boundary conditions such as spindle bearings.

This eliminates the need for extensive thermo-elastic investigations of the spindle and enables a scalable, efficient spindle correction tool. In addition, the spindle correction model can be coupled with a second model considering thermo-elastic effects coming from the machine tool's structure. For an industrial applicability of the modelling and correction methodology, it has to be shown that the knowledge gained can be transferred to a production machine.

Therefore, the following steps provide proof of the general functionality:

- Development of a white-box model used to parametrize a spindle correction model (chapter 3)
- Parametrization of a machine tool structure model based on experimental tests (chapter 4)
- Combination of both models and validation on a production machine (chapter 4)

3 WHITE-BOX PARAMETRIZATION OF A THERMO-ELASTIC SPINDLE CORRECTION MODEL

3.1 Structure of a white-box model for thermo-mechanical spindle deformations

The simulation environment for an externally driven spindle (Figure 1**Chyba! Nenalezen zdroj odkazů.**) consists of a thermal simulation and a mechanical simulation that operate independently and are coupled as co-simulation.

Figure 1: Exemplary externally driven spindle

As displayed in Figure 2, both FE models are optimized with respect to the demands of each simulation domain. While a mesh of linear tetrahedral elements is defined to calculate thermal effects, a Timoshenko beam mesh is designed to approximate the mechanical structural behavior. However, since only axial effects are considered in this paper, the results are not affected by the underling beam theory. An analytic-empirical model based on Hertzian theory considers nonlinear spindle bearing effects. In order to connect both simulation domains, calculated transient temperature fields are continuously mapped onto the beam mesh as thermal substitute forces.

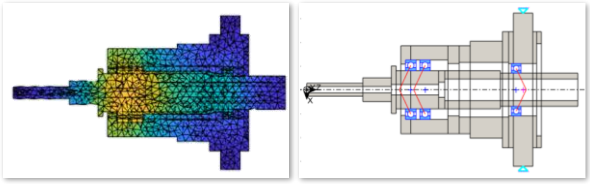

Figure 2: Schemas of thermal and mechanical simulation

3.2 Thermal simulation

Thermal boundary conditions (BC) in spindles are heat sources, heat sinks, and transfer coefficients. Besides geometric and material parameters, these BC define the thermal spindle behavior decisively. In externally driven spindles, frictional bearing losses happen to be the primary heat source, while fluid losses in air gaps lead to minor heat generation due to generally lower rotational speeds compared to motor spindles. Forced and free convection as well as minor heat transmission into the machine structure are the main heat sinks. The investigated spindle has two front and one rear bearing that are rigidly adjusted in an O-arrangement. All relevant thermal BCs and corresponding calculation models are described below.

Bearing friction

There are numerous approaches to calculate friction moments of spindle bearings. Due to the importance of accurately predicted bearing friction to simulate thermo-elastic deformations accurately, empirical investigations are performed on a spindle test rig (Figure 3).

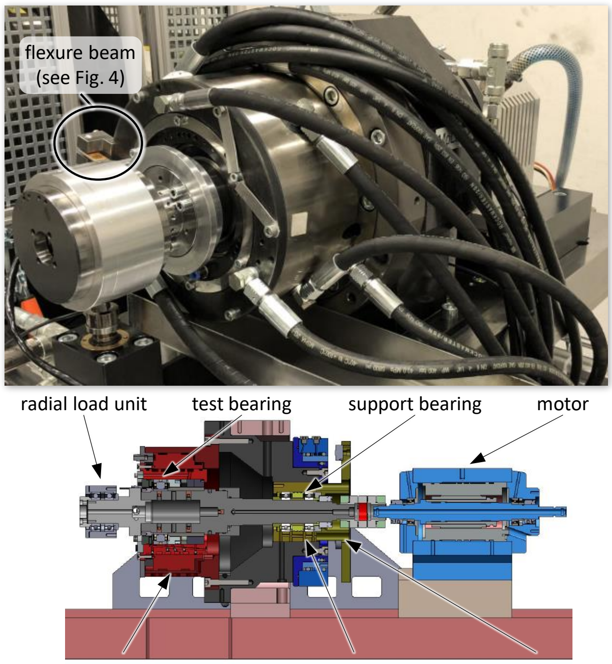

Figure 3: Spindle test rig

Therefore, the spindle bearings are mounted into a hydrostatically carried sliding bearing that itself is connected to the housing with a flexure beam. Onto the beam, a strain gauge is attached. The strain gauge is calibrated by applying discrete weights on the clamped beam and measuring the voltage transfer behavior of the strain gauge bridge. A linear function is derived (Figure 4).

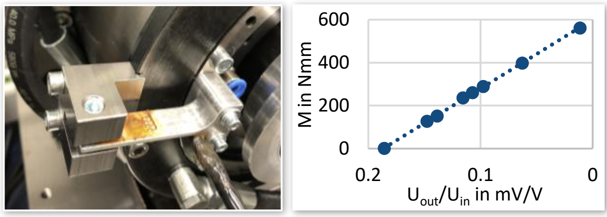

Figure 4: Flexure beam and calibrated transfer function

After that, the beam deflection can be transformed into the corresponding bending/friction moment. During the test, radial load is applied via a hydraulic actuator and static axial load can be induced through a hydrostatic axial bearing. A detailed description of the test rig is given in **[Falker 2020]**.

Figure 5 shows exemplary friction moments plotted against spindle speed for different discrete axial loads. Standard spindle bearings with steel balls are investigated. For different combinations of radial and axial loads, friction moments are measured and stored in tabular form.

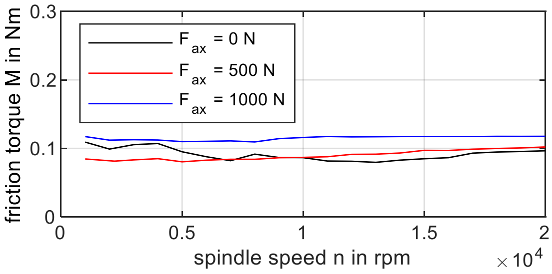

Figure 5: Stribeck curves for a spindle bearing

Convection

Convectional heat losses are described with existing empirical models based on theory of similarity **[VDI 2013]**. A calculation model for free convection of horizontal cylinders as well as a model for rotating shafts is used. For radiation, a convectional formulation with a temperature T varying heat transfer coefficient $\alpha_{radiation}$ is chosen (eq. 1 and 2). ϵ, σ and T_0 are the coefficient of emission, the Stefan–Boltzmann constant and the environmental temperature.

$$\dot{q}_{radiation} = \alpha_{radiation} \cdot (T - T_0) \quad (1)$$

$$\alpha_{radiation} = \epsilon \cdot \sigma \cdot (T^2 + {T_0}^2)(T + T_0) \quad (2)$$

Solid contacts

Heat conduction inside spindles is strongly affected by transfer resistances $R_{contact}$ of solid contacts such as bearing seats or the connection to the machine structure. In **[Bernhard 2014]**, these effects are considered using the effective pressure p, thermal conductivity of both partners λ_1 and λ_2 as well as surface conditions (roughness R_a, skew m and micro hardness H) as input values to calculate a heat transfer coefficient $\alpha_{contact}$ as output (eq. 3 and 4).

$$\alpha_{contact} = \frac{1}{R_{contact}} \quad (3)$$

$$R_{contact} = 0.46 \cdot \frac{R_a}{m} \cdot \left(\frac{1}{\lambda_1} + \frac{1}{\lambda_2}\right) \cdot \left(\frac{p}{H}\right)^{-0.93} \quad (4)$$

For bearing seats, the effective pressure is derived from assuming an ideal cylindrical compression connector, while a mean pressing is considered for screw connections by dividing the total screw forces through the connector area. Values for surface roughness are estimated based on the underlying finishing process resulting in surface roughness values R_a of 7.05, 1 and 0.11 µm for roughing, finishing and grinding.

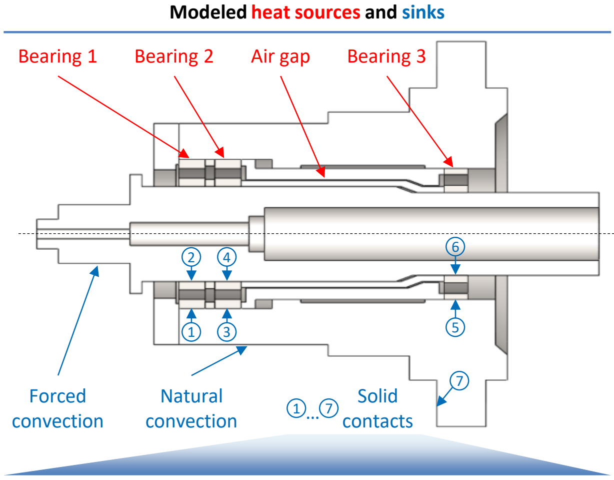

Position	1	2	3	4	5	6	7
HTC	10.2	22.1	10.2	22.1	10.3	22.1	1.4

Figure 6: Cross section, bearing setup and heat transfer coefficients of solid contacts in W/m²K

3.3 *Mechanical simulation*

The Timoshenko beam FE mesh coupled to nonlinear Hertzian bearing models allows calculating mechanical spindle characteristics such as elastic structure deformation, static and dynamic stiffness and bearing conditions like contact pressing or angle. Therefore, an iteratively operating solver converges to a state of equilibrium, where the sum of internal reactionary contact forces of each roller element equals the sum of external loads. For each roller element, the following forces and corresponding moments are considered:

- Normal forces
- Friction forces in rolling contacts
- Centrifugal forces
- Gyroscopic moments
- Normal and friction forces between roller elements and cage

During the solution process to find static equilibrium, contact angles are varied. In consequence, the relative position of inner and outer bearing rings is adjusted culminating in axial shaft displacements. The solution process is documented in **[Brecher 2019]**.

By integrating thermal substitute forces, thermo-mechanical interactions can be calculated. In the context of this work, two main influences on the spindle TCP position are considered:

1) Thermo-elastic axial spindle shaft expansion
2) Kinematic axial spindle shaft displacement

3.4 *Validation*

Thermo-mechanical simulation results are validated by comparing them to measured axial TCP deflection of the investigated spindle. In a step run of 30 minutes per step, spindle speed is increased over time. Maximum spindle speed is 10,000 rpm. Spindle rotation is interrupted every five minutes for a measurement. Therefore, spindle and dummy tool are moved towards an inductive displacement sensor nest according to **[ISO 230-3]** mounted on the fixed machine table (Figure 7).

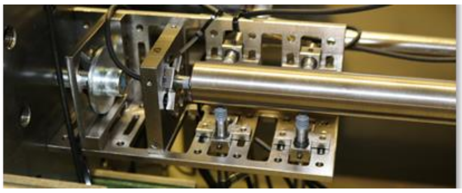

Figure 7: Measurement setup

Figure 8 shows high agreement between experimental and simulated data. The mean absolute error (MAE) is 1.33 µm.

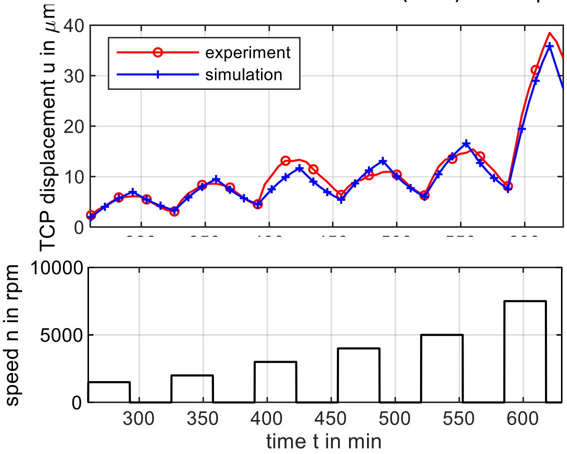

Figure 8: Calculated and measured axial spindle TCP position

3.5 Spindle correction model

In order to set up a spindle correction model, transient thermo-elastic TCP deflection Δu_{axial} is simulated for different, constant load cases (eq. 5). For each load case, a time-displacement curve follows. As described in 3.3, thermo-elastic as well as kinematic effects are considered.

$$\Delta u_{axial} = \Delta u_{thermal} + \Delta u_{kinematic} \qquad (5)$$

Thermo-elastic effects depend on different variables such as spindle speed n, axial load F_{ax}, and radial load F_{rad} (eq. 6).

$$\Delta u_{thermal} = \Delta u_{PT1_n} + \Delta u_{PT1_{F,ax}} + \Delta u_{PT1_{F,rad}} \qquad (6)$$

For constant spindle speed, the time course of axial displacement can be expressed as first order delay, where the corresponding coefficients K and T depend on n. Due to nonlinear bearing characteristics, it was found suitable to correlate respective coefficients with frictional bearing power losses $P(n)$ instead of spindle speed n (eq. 7).

$$\Delta u_{PT1_n}(t) = K\big(P(n)\big) \cdot \left(1 - e^{-\frac{t}{T(P(n))}}\right) \qquad (7)$$

As a results, the nonlinear effects remain in the bearing friction tables (friction as function of spindle speed) and for the coefficients linear correlations arise (Figure 9). The functional correlation is derived from simulating time courses for different spindle speeds and fitting respective parameters. Figure 9 shows the linear correlation between K and T and power loss P.

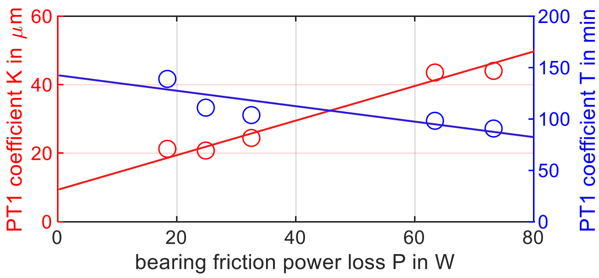

Figure 9: PT1 coefficients K and T as function of bearing power losses

The linear functions for K and T are given in eq. 8 and 9.

$$K(P) = 0.4817 \cdot P + 10.3617 \qquad (8)$$

$$T(P) = -0.6298 \cdot P + 135.245 \qquad (9)$$

By inserting equations 8 and 9 into 7, spindle speed influence on thermo-elastic axial TCP displacement can be calculated as a function of time. P as a function of spindle speed is defined by the measured Stribeck curves. The procedure to consider other variables such as radial or axial load is equivalent.

Beside thermo-elastic effects, kinematic effects are taken into account. Therefore, axial spindle displacement is calculated for different spindle speeds (Figure 10). Due to a rigidly adjusted bearing arrangement and the fact that two front bearings are mounted against just one rear bearing, the spindle shows significant kinematic displacements. Centrifugal forces in angular contact bearings make the steel balls move up the curvature radius of the bearing track. This results in an axial movement and in a deceasing contact angle.

The curve shows an inflection point caused by two inverse effects under rising spindle speed:

1) Increasing centrifugal forces → increasing axial displacement
2) Decreasing contact angles → decreasing axial displacement

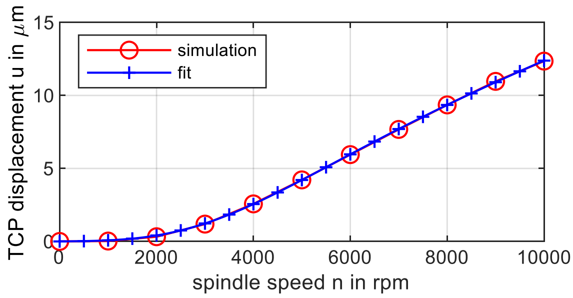

Figure 10: Kinematic axial spindle shaft displacement

Thus, the kinematic TCP displacement can be approximated with an analytic function considering both effects. On the one hand, centrifugal force has a quadratic relationship with spindle speed n. On the other hand, the contact angle can reach a minimum of zero (which is equivalent to no axial force). Defining an exponential function with an exponent approaching zero for big rotational speeds allows a precise approximation (eq. 10).

$$\Delta u_{kinematic,fit} = 1.28E\text{-}3 \cdot n^{1-6.97E\text{-}1 \cdot e^{-5.3E\text{-}4 \cdot n}} \qquad (10)$$

MAE of the analytic model is 0.023 µm. By coupling the kinematic correction model with the previously introduced thermo-elastic model, a full thermo-mechanical spindle correction is achieved.

4 EXPERIMENTAL VALIDATION OF THE COUPLED CORRECTION MODEL

4.1 Experimental machine and the measuring setup

The validation is carried out on a horizontal 4-axis machining center with [*wBZ'bXYt*] kinematics according to **[ISO 10791-6]** (annex B). The displacement of the machine is recorded by the ETVE test according to **[ISO 230-3]**. In addition, measuring rods are placed on the table, which measure the displacement of the spindle flange at four points (Figure 11). The points are placed from the spindle center in positive and negative directions along the X and Y axis. The measurement of the machine displacement includes five degrees of freedom, while three degrees of freedom of the spindle displacement are determined.

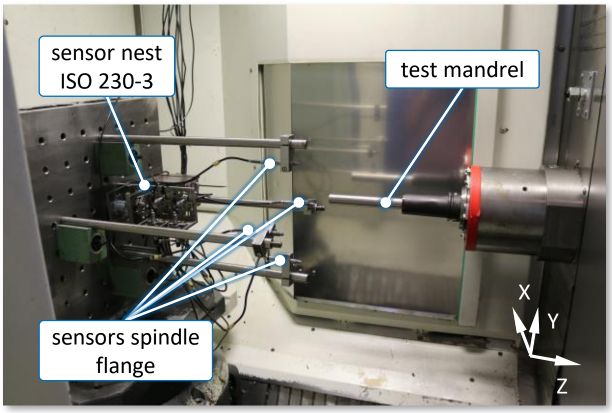

Figure 11: Measurement setup

The measuring rods, the measuring nest and the measuring mandrel are made of invar due to its particularly low thermal expansion coefficient. The evaluation is based on the assumption that the invar (iron-nickel alloy) measurement equipment does not deform thermo-elastically ($\alpha_{th} = 1.7 \frac{10^{-6}}{K}$). In addition, four sensors record ambient temperatures. Three sensors are placed outside the machine and one sensor is suspended in the working area.

In order to prove the suitability of the measuring setup, a test was carried out on the repeatability of approaching the sensors. Therefore, the spindle was moved into the measuring setup five times. The sensor raw data is averaged over two seconds for each test. According to [JCGM 2008], this resulted in a maximum fluctuation of ±2σ = ±0.55 µm for the average values.

4.2 Validation of the machine model

Besides the thermo-elastic behavior of the main spindle, the kinematic of the machine also shows relevant transient displacements [Mayr 2012]. The modelling of machine behavior was a field of intensive research since the 1960's. [Wissmann 2014] offers a detailed overview of the field. The effects of spindle and kinematics are recorded separately by the measurement setup presented in 2.4. In order to compensate for both effects, superposed corrections are used in this paper without mapping a possible interaction.

Figure 12 shows the structure of the machine model. It is divided into two submodels for the internal and external thermo-elastic influences on the machine (eq. 11).

$$\Delta u_{machine} = \Delta u_{internal} + \Delta u_{external} \tag{11}$$

The model for the internal influences uses as a starting function already successfully applied first-order delay elements (eq. 7). Model input variables in literature are generally internal machine data and for this work the axis feed rate. The models ability to map the behavior of a complete kinematic is well proven in literature. For this paper the internal influences are represented by the X-axis, as the focus lies on the reduced parametrization of the spindle model and the general coupling of the experimentally validated model with the virtually validated model [Mayr 2012, Wissmann 2014, Wennemer 2017].

The submodel for the external influences, e. g. the environmental influences, uses the same function. The input variable here is the average value of the changes of the ambient temperature at the four ambient temperature sensors $\overline{\Delta T_{ambient}}$, see 4.1 [Gebhardt 2014, Wissmann 2014, Wennemer 2017].

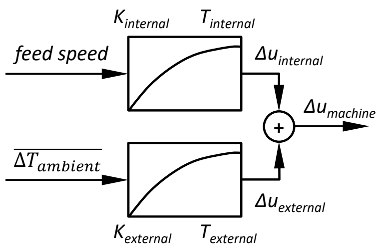

Figure 12: Structure of the machine model

Figure 13 shows the measured error, the calculated machine model with the submodels for internal and external influences, the residual error, calculated as the difference between measurement and machine model, and the model input variables.

The machine model reduces the maximum error of 16.9 µm by at least 78% to 3.8 µm. The mean square of the model deviation is 1.5 µm.

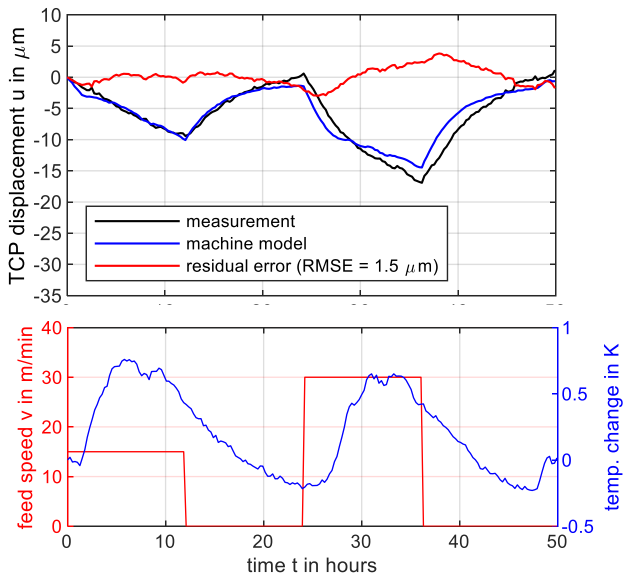

Figure 13: Machine model including axis load and environmental load

4.3 Validation of the combined correction model

In Figure 14, validation results are presented. During a 45-hour run, spindle speed as well as feed axis speed have been varied independently. The calculated course represents the combined model results consisting of a spindle part and a machine part. Overall, the hybrid parametrized correction model significantly improves the TCP accuracy, although still notable deviations between model and reality occur. Especially the heating process of the main spindle is not approximated with the necessary accuracy, resulting in correction errors during the first spindle steps of each block (e.g. hour 30). A possible reason is that only individual bearings were investigated on the test rig and spindle bearing arrangements are not considered.

Furthermore, external and highly instationary effects like an open hall gate (at hour 17) can not be taken into account in detail. Here, more flexible environment models need to be developed [Brecher 2018].

It can be summarized that the combination of a white-box based spindle correction model (FE simulation) and a black-box based machine correction model (experiments) enables a more time-efficient and precise correction strategy then the actual state of industry.

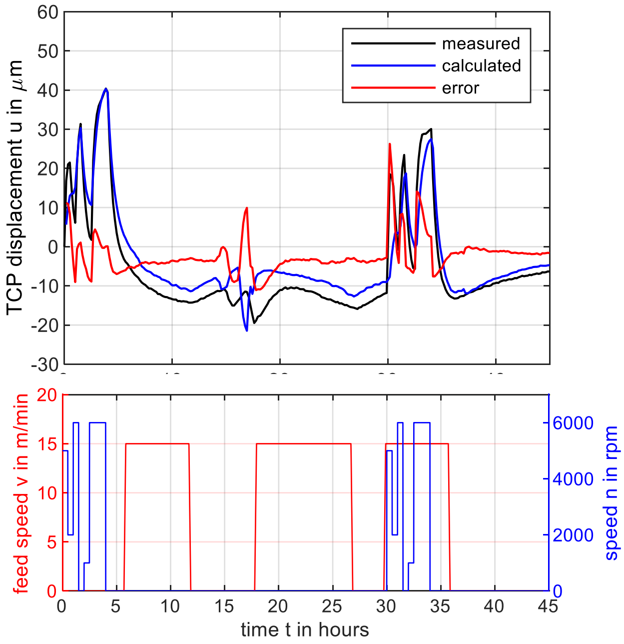

Figure 14: Validation results

5 CONCLUSION AND OUTLOOK

This work presents a new hybrid approach to reduce the necessary experimental parametrization effort for correction approaches of thermo-elastic effects in machine tools. On the example of an externally driven spindle, a simulation model (white-box) containing phenomenological knowledge is used to parametrize a correction model.

This white-box spindle model combined with an experimental parametrized machine model (black-box) for internal and external thermal loads form a new hybrid modelling approach to reduce thermo-elastic TCP errors.

The key advantage of the developed correction method is a significant reduction of parametrization time, since the major part of parametrization data is generated virtually. Cost-intensive on-machine experiments are drastically minimized. When considering spindle speed, axial load and radial load as main factors influencing the thermo-elastic behavior, the experimental parametrization effort can be assumed with multiple days per spindle unit. Furthermore, a once defined model cannot be transferred to a new spindle. By using the new approach, the virtual prototype allows avoiding cost-intensive on-machine experiments by still considering the complex and nonlinear thermo-elastic behavior.

Future work should focus on extending the spindle test rig to analyze different spindle arrangements. In addition, more detailed models are required to include the common industrial environment of a production machine such as an open hall gate. Finally, the influence of stacking different individual models needs to be investigated more deeply to improve the overall accuracy of the presented correction methodology.

ACKNOWLEDGEMENT

The Authors would like to thank the German Research Foundation (DFG) for financial support. The presented findings result from the transfer project T01 within CRC/TRR 96 - Project-ID 174223256 – TRR 96 “Thermo-Energetic Design of Machine Tools”.

REFERENCES

[Bernhard 2014] Bernhard, F.: Handbuch der Technischen Temperaturmessung, Springer Berlin Heidelberg, 2014.

[Böttger 1994] Böttger, J.: Hydrostatisch gelagerte Präzisions-spindeln – Möglichkeiten zur thermischen Stabilisierung. ISBN: 3-8265-0010-5. Thesis, RWTH Aachen, 1994.

[Brecher 2018] Brecher, C.; Kneer, R.; Spierling, R.; Frekers, Y.; Fey, M.: Ein Beitrag zur Modellierung des thermischen Umgebungseinflusses an Werkzeugmaschinen. In: ZWF - Zeitschrift für wirtschaftlichen Fabrikbetrieb. 113. September, 2018.

[Brecher 2019] Brecher, C.; Falker, J.; Fey, M: Simulation schnell drehender Welle-Lager-Systeme - Teil 1. In: Antriebstechnik. Vol. 58, Issue 6, pp. 66-72.

[Brecher 2020] Brecher, C.; Steinert, A.; Neus, N.; Fey, M.: Metrological investigation and simulation of thermo-mechanical interactions in externally driven spindles. In: Special Interest Group: Thermal Issues. 28. February 2020, Aachen

[Dehaes 1998] Dehaes, J.: Studie over de thermische Beinvloeding van de Bewerkingsnauwkeurigheid von een Freesmachine. Thesis, Katholieke Universiteit Leuven, 1998.

[Falker 2020] Falker, J.: Analyse des Betriebsverhaltens von Hochgeschwindigkeits-Wälzlagern unter radialen Lasten. ISBN: 978-3-86359-799-3.Thesis, RWTH Aachen, 2020.

[Gebert 1997] Gebert, K.: Ein Beitrag zur thermischen Modell-bildung von schnelldrehenden Motorspindeln. ISBN: 978-3826528811. Thesis. Technische Hochschule Darmstadt, 1997.

[Gebhardt 2014] Gebhardt, M. et al.: High precision grey-box model for compensation of thermal errors on five-axis machines. CIRP Annals, Vol. 63, Issue 1, pp. 509-512, ISSN: 0007-8506

[Gleich 2008] Gleich, S.: Simulation des thermischen Verhaltens spanender Werkzeugmaschinen in der Entwurfsphase. ISBN: 978-3-937524-77-1. Thesis. Technische Universität Chemnitz, 2008.

[Harris 1991] Harris, T. A.: Rolling Bearing Analysis. 3rd edition, New York: John Wiley & Sons, 1991. ISBN 978-0471513490

[Heisel 1980] Heisel, U.: Ausgleich thermischer Deformationen an Werkzeugmaschinen. ISBN: 3-446-13083-7. Thesis, TU Berlin, 1980.

[Heisel 1997] Heisel, U.; Stehle, T.: Fuzzy-Logik zur Bestimmung des thermischen Verhaltens. Die Maschine – dima – digitale maschinelle Fertigung, Band 51, Heft 10/11, 1997.

[Heisel 2011] Heisel, U.; Rothmund, J.; Jakob, P., Böhm, T. Spindelmodell zur dynamischen FEM-Simulation. ZWF – Zeitschrift für wirtschaftlichen Fabrikbetrieb, 2011, Vol. 106, No. 4, pp. S. 245-248. ISSN 0947-0085.

[Holkup 2010] Holkup, T., Cao, H., Kolar, P., Altintas, Y., Zeleny, J: Thermo-mechanical model of spindles. CIRP Annals, Vol. 59, Issue 1, pp. 365-368.

[Hu 2013] Hu, J.: Modellierung und Simulation des thermischen Verhaltens einer Werkzeugmaschine. ISBN: 978-3-8396-0660-5. Thesis. Technische Universität Berlin, 2013.

[ISO 10791-6] ISO 10791-6:2014(E) Test conditions for machining centres - Part 6: Accuracy of speeds and interpolations. ISO copyright office, Genf, 2014.

[ISO 230-3] ISO 230-3:2007(E) Test code for machine tools – Part 3: Determination of thermal effects. ISO copyright office, Genf, 2007.

[JCGM 2008] JCGM 100:2008 Evaluation of measurement data – Guide to the expression of uncertainty in measurement

[Jedrzejewski 2008] Jedrzejewski, J.; Modrzycki, W.; Kowal, Z.; Kwasny, W.: Precise Modelling of HSC Machine Center for Aerospace Parts Machining. Journal of Machine En-gineering, 2008, Vol. 8., Issue 3, pp. 29–41.

[Kim 2004] Kim, K-D., Kim, M-S., Chung, S-C.: Real-Time Compensatory Control of Thermal Errors for High- Speed Machine Tools. In: Proceedings of the Institution of Mechanical Engineers, Part B: Journal of Engineering Manufacture, Vol. 218, No. 8, 1. August 2004. pp 913-924, DOI: 10.1243/0954405041486163.

[Kreis 2008] Kreis, M.: Zum Eigenverhalten von Motorspindeln unter Betriebsbedingungen. ISBN: 978-3832274351. Thesis. Technische Universität Darmstadt, 2008.

[Li 2004] Li, H.; Shin, Y. C.: Integrated Dynamic Thermo-Mechanical Modeling of High Speed Spindles, Part 1. Journal of Manufacturing Science and Engineering. Vol. 126, Issue 1, pp. 148-158.

[Ma 2016] Ma, C.; Zhao, L.; Shi, H.; Mei, X.; Yang, J.: Experi-mental and simulation study on the thermal characteristics of the high-speed spindle system. Journal of Mechanical Engineering Science 2017, Vol. 231, Isssue 6, pp. 1072-1093.

[Mares 2013] Mares, M.; Horejs, O.; Hornych, J.: Robustness and Portability of Machine Tool Thermal Error Compensation Model based on Control of participating Thermal Sources. Journal of Machine Engineering, January 2013, Vol. 13, No. 1, pp 24-36, ISSN 1895-7595.

[Mayr 2012] Josef Mayr et al.: Thermal issues in machine tools. CIRP Annals, Vol. 61, Issue 2, 2012, pp. 771-791, ISSN 0007-8506

[Roissant 2013] Rossaint. J.: Steigerung der Leistungsfähigkeit von Spindellagern durch optimierte Lagergeometrien. ISBN: 978-3-86359-169-4. Thesis, RWTH Aachen, 2013.

[SKF 2013] SKF: Rolling bearings. Company publication, 2013.

[Spur 1986] Spur, G.; Hoffmann, E.; Suppanz, N.: Eine Methode zum Ausgleich thermisch bedingter axialer Spindel-verlagerungen an numerisch gesteuerten Werkzeugmaschinen. ZWF – Zeitschrift für wirtschaftlichen Fabrikbetrieb, 1986, No. 11, pp. 645-651, ISSN: 0932-0482.

[Steinert 1995] Steinert, T.: Das Reibmoment von Kugellagern mit bordgeführtem Käfig. ISBN: 3-8265-1210-3.Thesis, RWTH Aachen, 1995.

[Tönshoff 1990] Tönshoff, H.-K.; Wulfsberg, J.-P.: Compensation of thermal induced displacements in machine tools. In: Proc. of Manufacturing International ’90, Vol. 5, 25-28. March 1990. Atlanta: pp 41-50, ISBN: 978-0791804704.

[VDI 2013] Gesellschaft Verfahrenstechnik und Chemieingenieurwesen: VDI-Wärmeatlas, Vol. 11, Berlin, 2013.

[Weck 2000] Weck, M.; Tüllmann, U.; Butz, F.: Schrägkugellager – Maschinenelement zur Lagerung schnell-drehender Spindel. Tagungsband: Gestaltung von Spindel-Lager-Systemen, WZL RWTH Aachen, 2000.

[Wennemer 2017] Wennemer, M.: Methode zur messtechnischen Analyse und Charakterisierung thermo-elastischer Verlagerungen von Werkzeugmaschinen. ISBN: 978-3-86359-592-0.Thesis, RWTH Aachen, 2017.

[Wissmann 2014] Wissmann, A.: Steuerungsinterne Korrektur thermisch bedingter Strukturverformungen von Bearbeitungs-zentren. ISBN: 978-3-86359-219-6. Thesis, RWTH Aachen, 2014.

[Wuldsberg 1991] Wulfsberg, J. P.: Diagnose und Kompensation thermischer Verlagerungen in Schleifmaschinen. ISBN: 9783181460085. Thesis, Universität Hannover, 1991.

[Zahedi 2012] Zahedi, A., Movahhedy, M. R.: Thermo-mechanical modeling of high speed spindles. Scientia Iranica, Vol. 19, Issue 2, pp. 282-293.

CONTACTS:

Alexander Steinert, M. Sc.
Laboratory for Machine Tools and Production Engineering (WZL) of RWTH Aachen University
Campus-Boulevard 30, 52074 Aachen, Germany
+49 241 80 28220, a.steinert@wzl.rwth-aachen.de, https://www.wzl.rwth-aachen.de